DE LA RECHERCHE À L'INDUSTRIE

Focusing, Post-acceleration and Bunching of TNSA protons with micro-helical coils

September 30th,2021

A. Hirsch[1,2], J. G. Moreau[1], L. Romagnani[3], C. Rousseaux[4], M. Ferri[1], F. Lefevre[3], I. Lantuéjoul[4], B. Etchessahar[1], S. Bazzoli[4], S. Chen[3], M. Chevrot[3], E. Loyez[3], E. Veuillot[3], W. Cayzac[4], B. Vauzour[4], B. Boutoux[4], L. Gremillet[4,5], R. Nuter[2], J. Fuchs[3], V. T. Tikhonchuk[2,6], E. D'Humières[2] et M. Bardon[1]

1) CEA-CESTA, France, 2) CELIA, University of Bordeaux-CNRS-CEA, France, 3) LULI, CNRS-Ecole Polytechnique-CEA, France, 4) CEA-DIF, France
5) LMCE, Paris-Saclay University-CEA, France, 6) ELI-Beamlines, Institute of Physics CAS, Czech Republic

Outline

- Motivations and phenomenology
- Experimental set-up
- Reminder of PACMAN 1 results
- PACMAN 2 parametrical studies
- Robustness study
- Conclusion and perspectives for PACMAN 3 and PETAL shots

Target Normal Sheath Acceleration (TNSA)

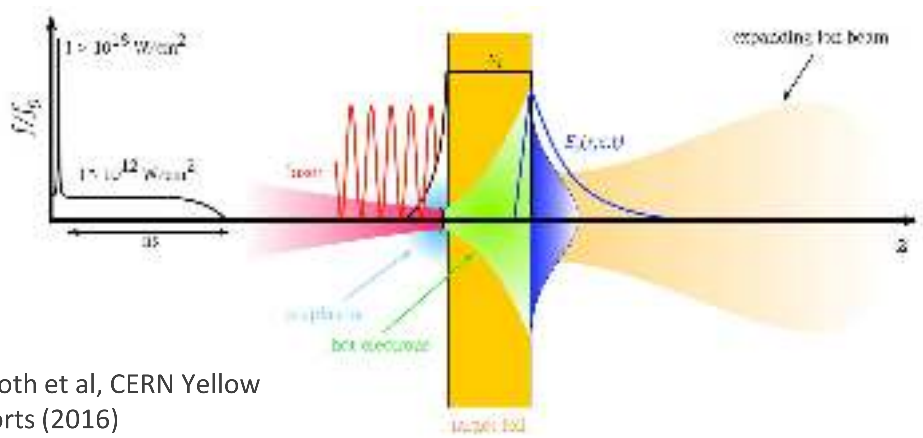

M. Roth et al, CERN Yellow Reports (2016)

The Target Normal Sheath Acceleration (TNSA) produces a proton beam with a large divergence angle (~40°) and energy bandwidth

Micro-helical Targets

Principle

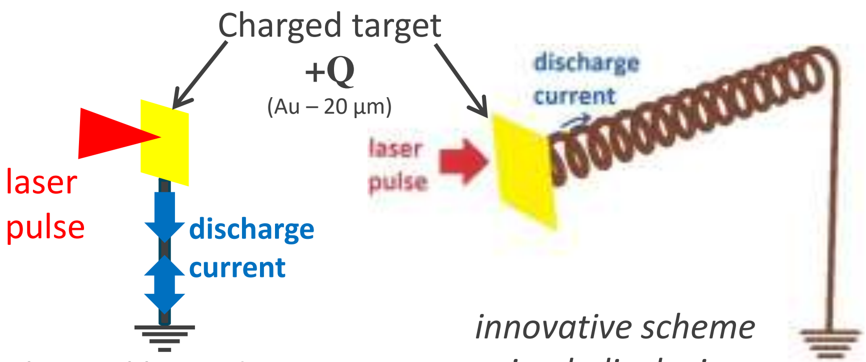

classical laser-driven ion acceleration scheme with vertical target holder

innovative scheme using helical wire holder (~ 10 mm long ; ~ 1 mm diameter)

target charging

discharge current pulse generation & propagation

local EMP generation

proton focusing and acceleration, and bunching

Proton beam and current pulse in the helical wire must be synchronized (0 order approximation)

$$\frac{p}{v_p} = \frac{\sqrt{p^2 + \pi^2 D^2}}{c}$$

$$\pi D < c\tau_{courant}$$

S. Kar, Nature Comm. (2016)

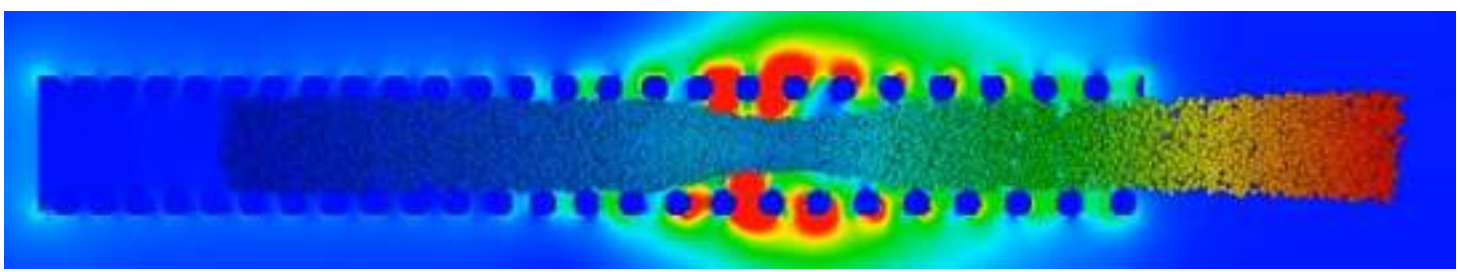

SOPHIE (CEA PIC simulation code) simulation of PACMAN

For the design of micro-helical targets, the 0-order is not enough

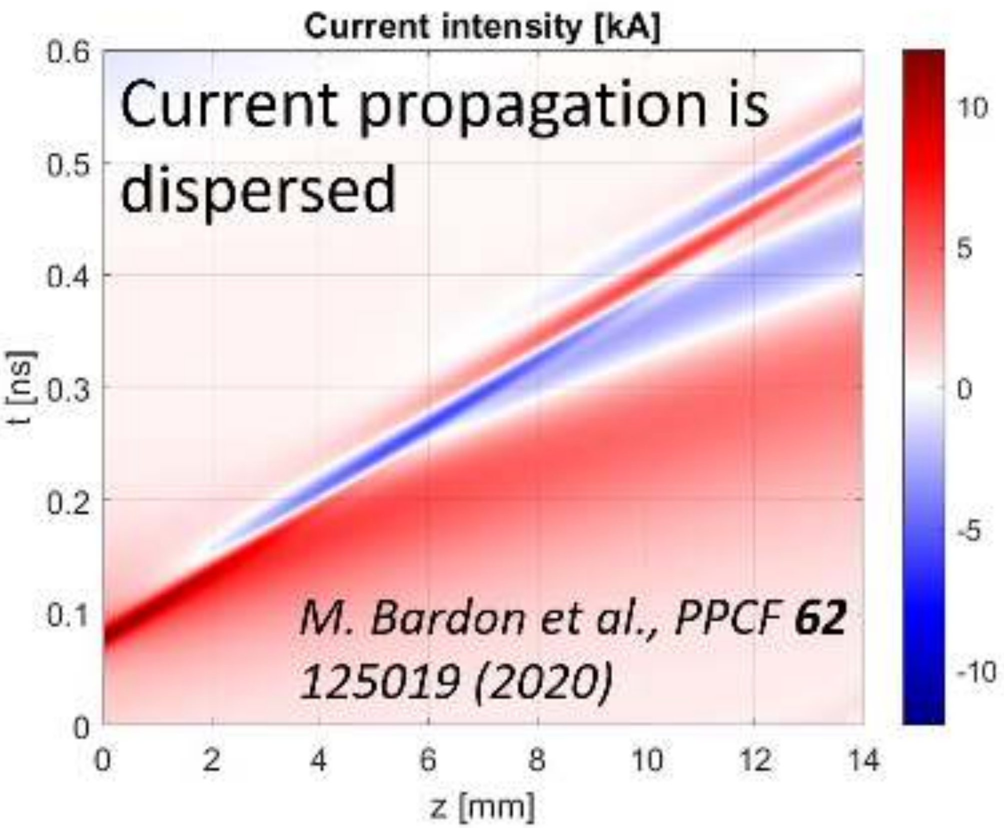

- We developed a numerical model based on traveling wave tubes theory (Kino G S and Paik S F 1962 *J. Appl. Phys.* **33** 3002), presented by Matthieu Bardon in the next poster session

⇒ Future targets to be designed with an optimisation algorithm applied to this model

Outline

- Motivations and phenomenology
- **Experimental set-up**
- Reminder of PACMAN 1 results
- PACMAN 2 parametrical studies
- Robustness study
- Conclusion and perspectives for PACMAN 3 and PETAL shots

Experimental Set-Up on LULI2000

<u>Laser parameters of PICO2000 (at LULI)</u>

35-50J on target, 1.3ps, 10^{19} W/cm^2, λ=1.053µm

2 campaigns: PACMAN 1 (march 2019) – PACMAN 2 (February 2020)

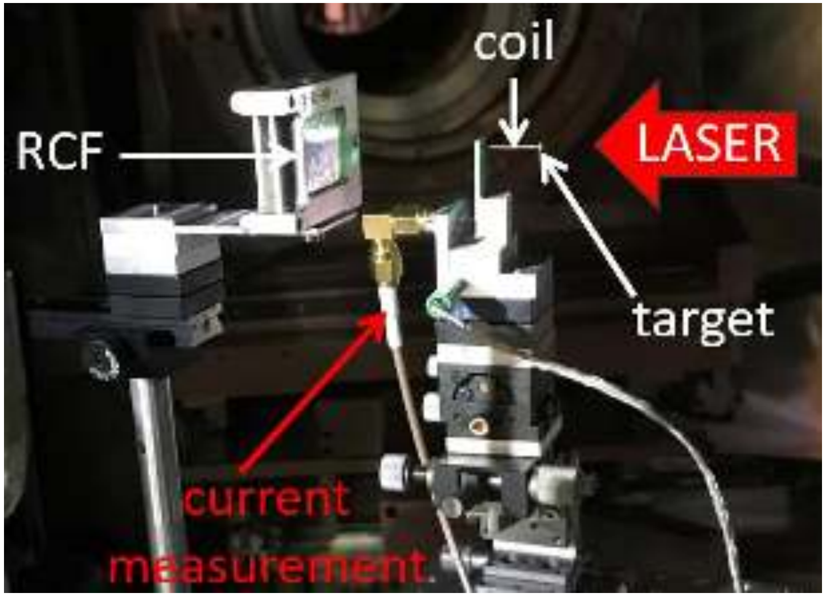

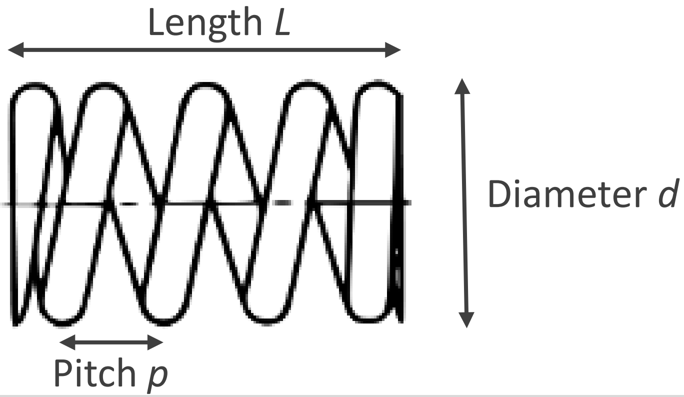

Experiment A

Experiment B

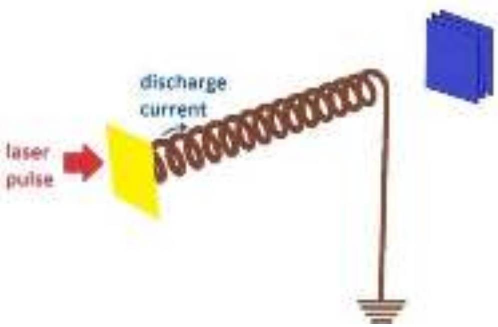

$\Rightarrow$ Compare the proton angular distribution and spectrum with/without the coil

Outline

- Motivations and phenomenology
- Experimental set-up
- **Reminder of PACMAN 1 results**
- PACMAN 2 parametrical studies
- Robustness study
- Conclusion and perspectives for PACMAN 3 and PETAL shots

Reminder of PACMAN 1 results

Experimental spectra for a shot with a coil of diameter *d=1.2mm*, pitch *p=0.35mm* and length *L=15mm* and for classical TNSA

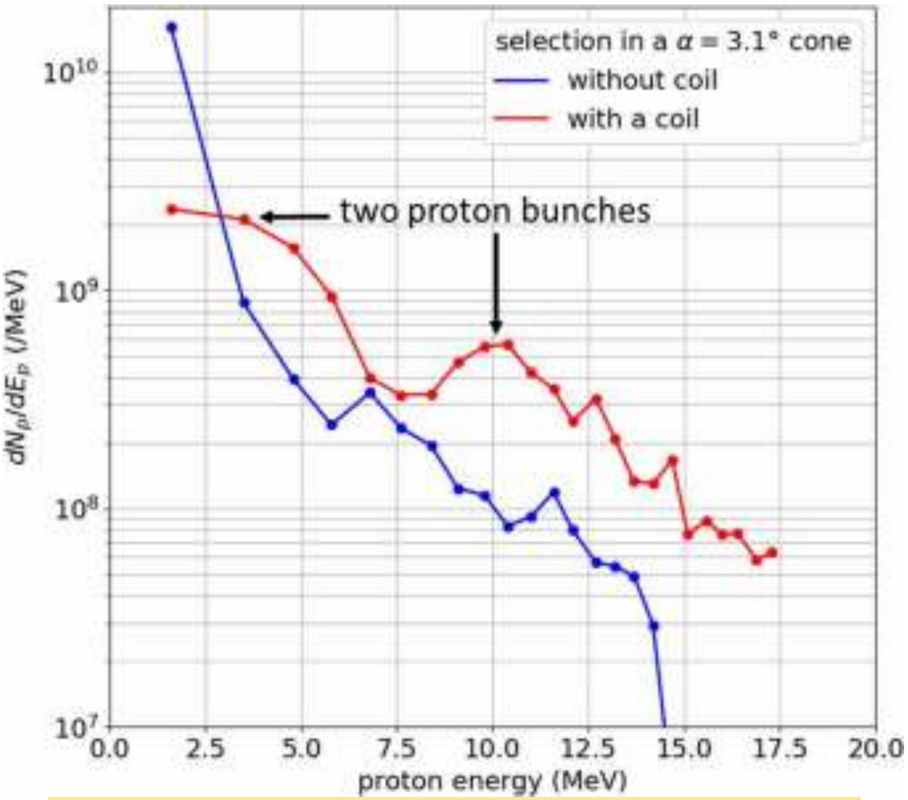

-Bunching of protons
-Increase of the maximum proton energy
-Strong focusing, charge can be multiplied up to a factor 7

M. Bardon *et al.*, Plasma Phys. Control. Fusion 62 (2020) 125019

Experimental and simulated spectra for a shot with a coil of diameter *d=1.2mm*, pitch *p=0.35mm* and length *L=15mm*

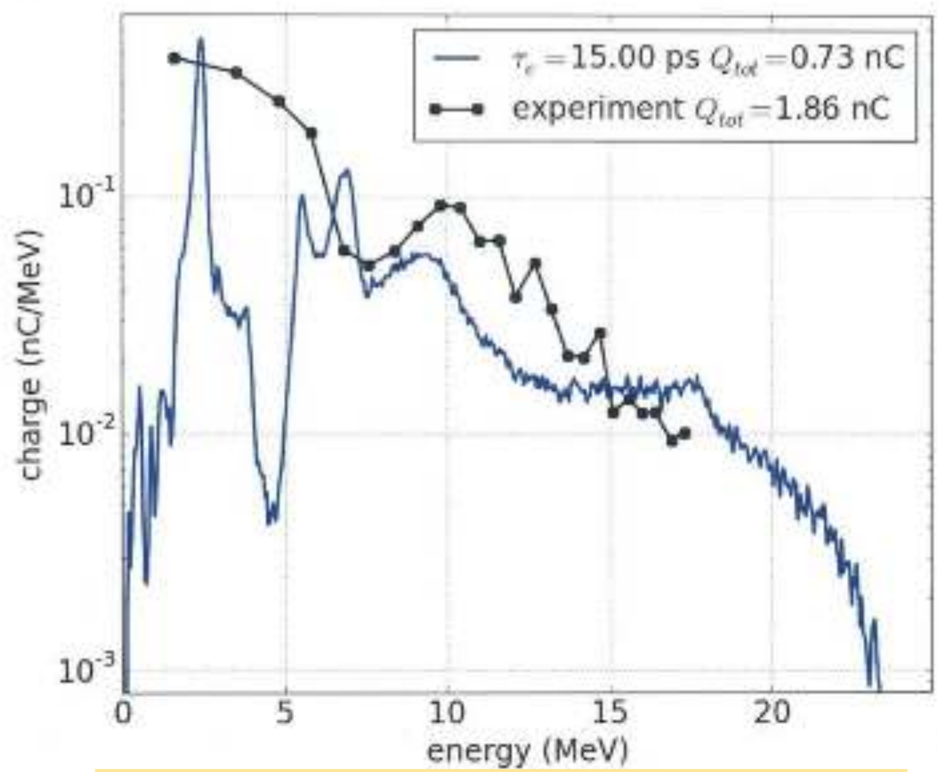

- Use of PIC code SOPHIE to retrieve our experimental results
- Proof of good agreement between experimental and simulated spectra on several coil geometries

Outline

- Motivations and phenomenology
- Experimental set-up
- Reminder of PACMAN 1 results
- **PACMAN 2 parametrical studies**
- Robustness study
- Conclusion and perspectives for PACMAN 3 and PETAL shots

Results of PACMAN 2

Without coil

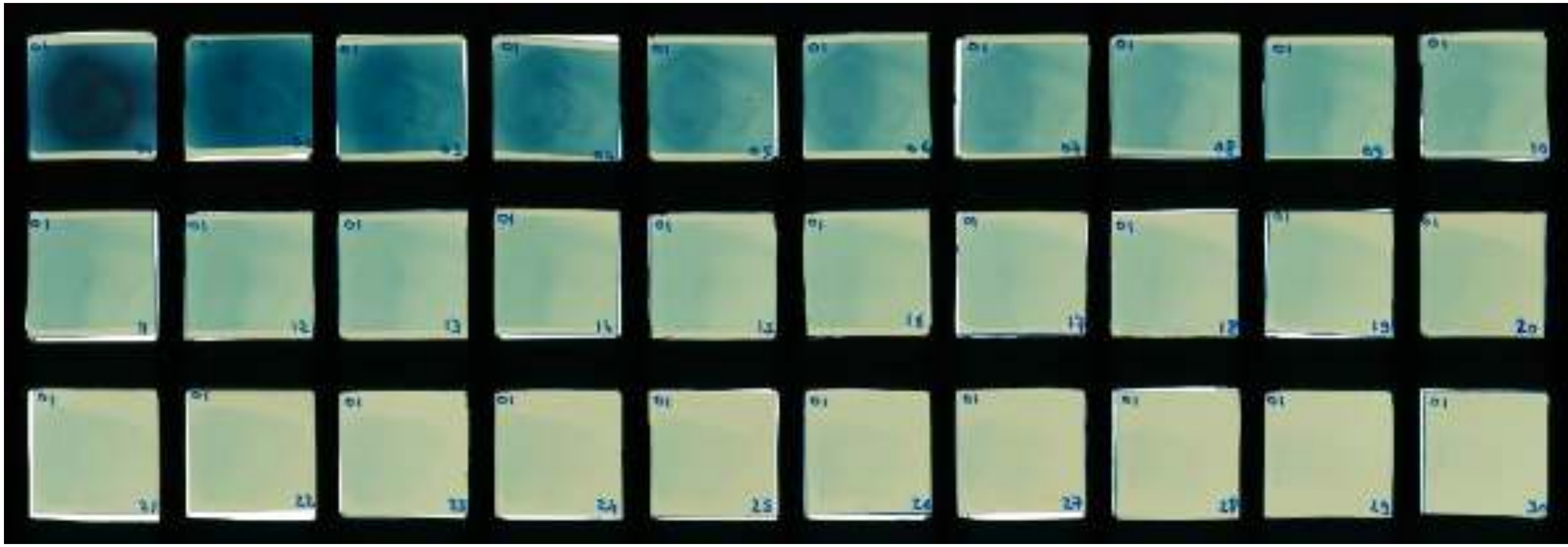

With coil

p=0.4mm
L=16mm
d=1.4mm

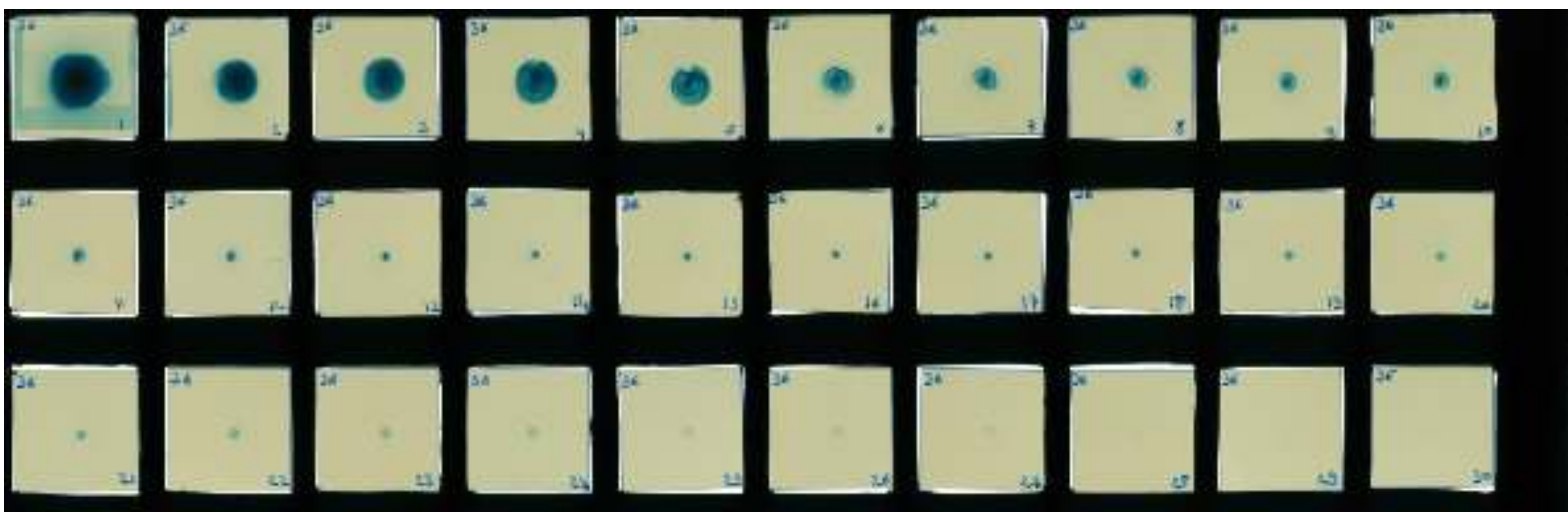

Results of PACMAN 2

Without coil

With coil
p=0.4mm
L=16mm
d=1.4mm

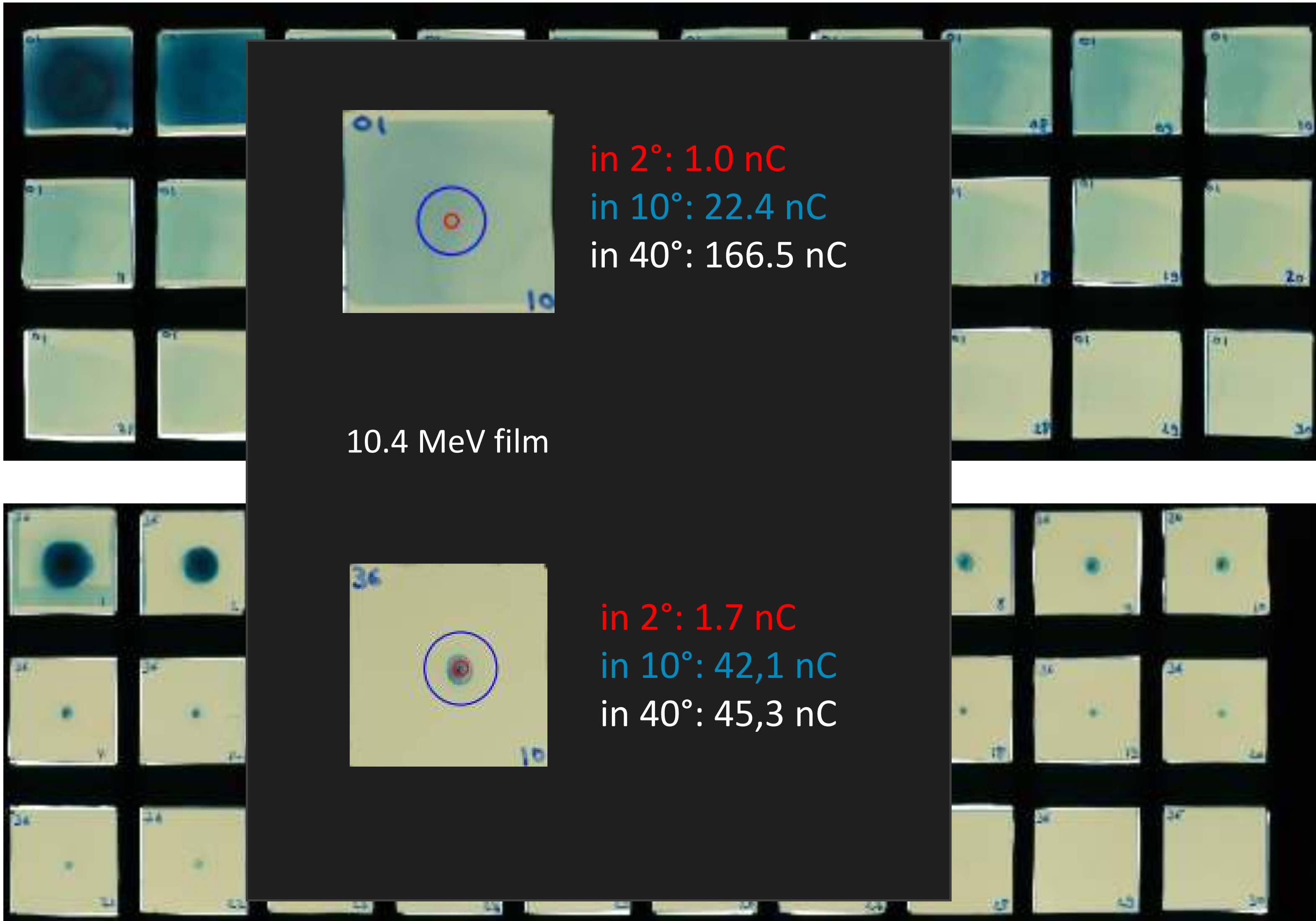

Parametrical studies: coil length variation

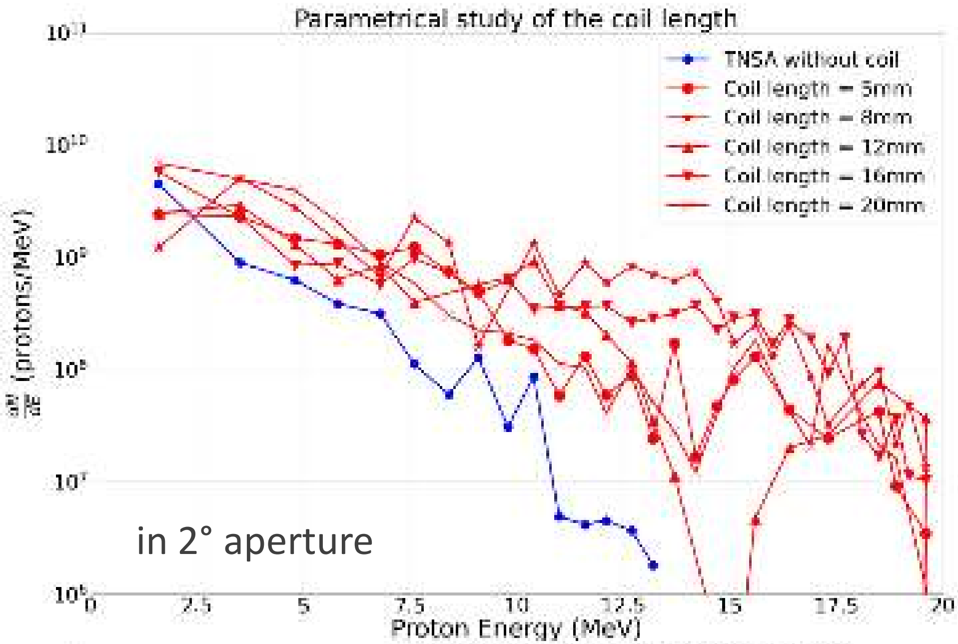

Experimental shots – p=0,4mm, d=1,2mm

- Cut-off energy over 20MeV for all coil lengths, at least 50% higher than TNSA shots
- We cannot see the impact of coil length on the cut-off energy due to the lack of sensibility of RCF at high energies in this regime
- Bunches at lower energies are not visible due to the lack of resolution over the first few RCF

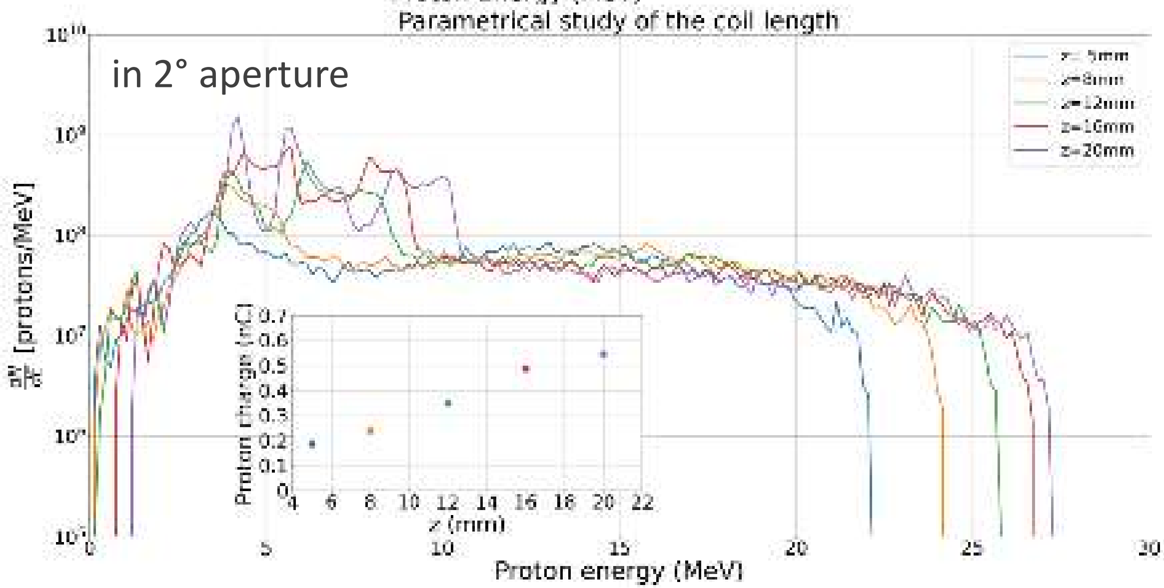

PIC simulations – p=0,4mm, d=1,2mm

- Increase of the cut-off energy with the coil length in the simulation
- Low energy bunches formed for L≥12mm
- Increase of charge inside the 2° cone when L increases

Parametrical studies: coil length variation

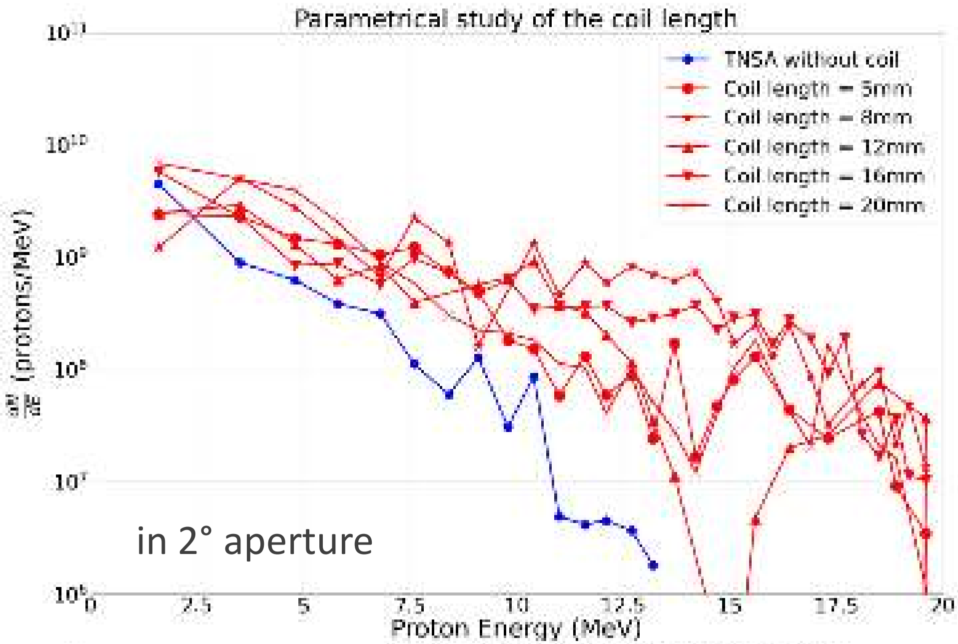

Experimental shots – p=0,4mm, d=1,2mm

- Cut-off energy over 20MeV for all coil lengths, at least 50% higher than TNSA shots
- We cannot see the impact of coil length on the cut-off energy due to the lack of sensibility of RCF at high energies in this regime
- Bunches at lower energies are not visible due to the lack of resolution over the first few RCF

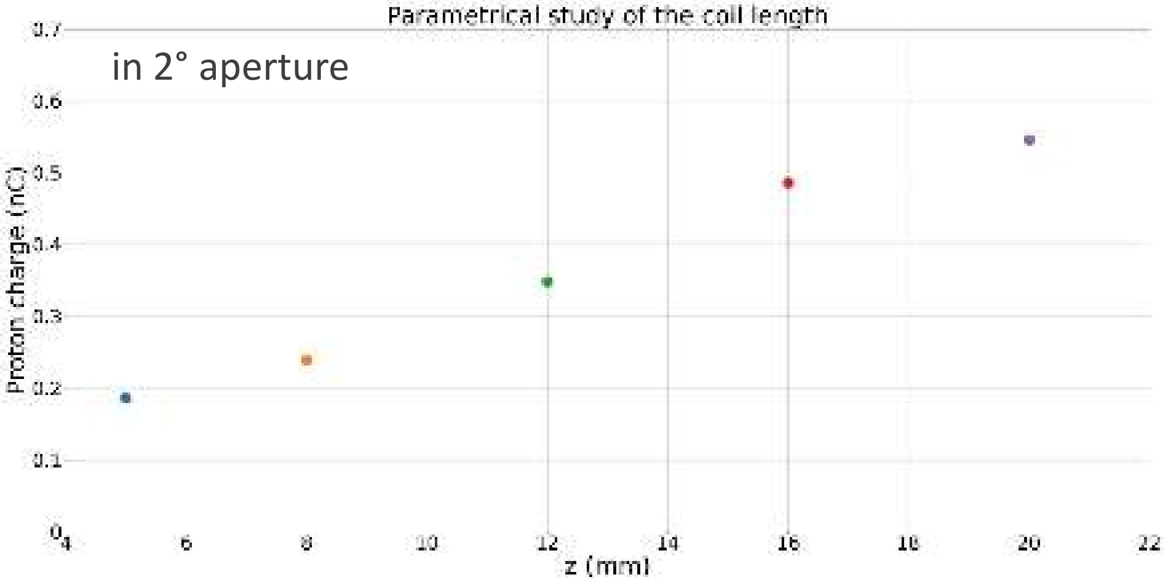

PIC simulations – p=0,4mm, d=1,2mm

- Increase of the cut-off energy with the coil length in the simulation
- Low energy bunches formed for L≥12mm
- Increase of charge inside the 2° cone when L increases

Parametrical studies: coil diameter variation

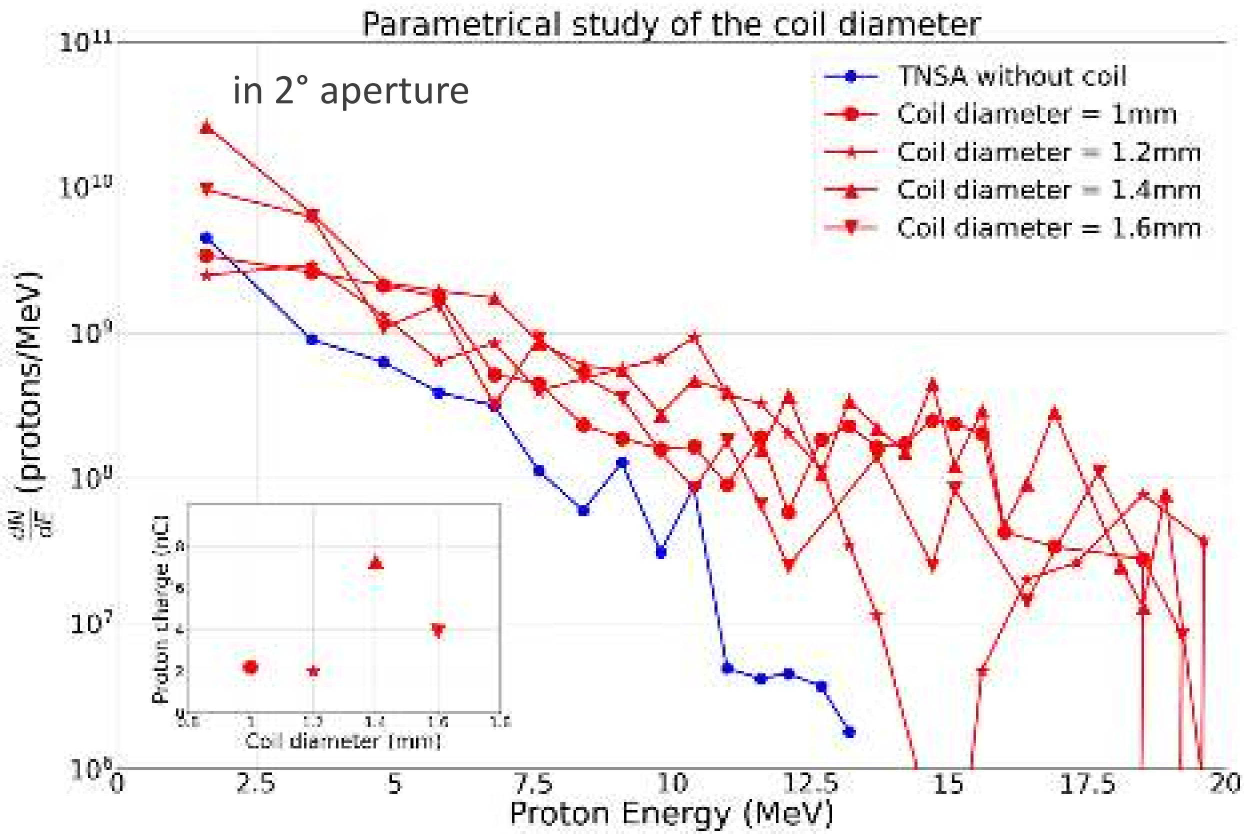

Experimental shots – p=0,4mm, L=16mm

- Spectrum of similar shape between different diameters
- Difference in the charge through the 2° cone:
  - ⇒ Maximum charge at d=1.4mm
  - ⇒ Equilibrium between proton injection and EM fields strength

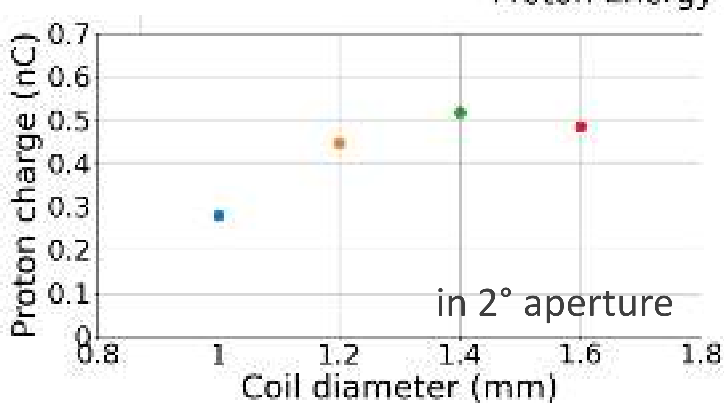

PIC simulations – p=0,4mm, L=16mm

- Qualitative agreement between experiments and simulations on the optimum diameter for proton charge
⇒ Numerical model will be used to find the optimal diameter for each coil pitch (cf poster M. Bardon)

Parametrical studies: coil diameter variation

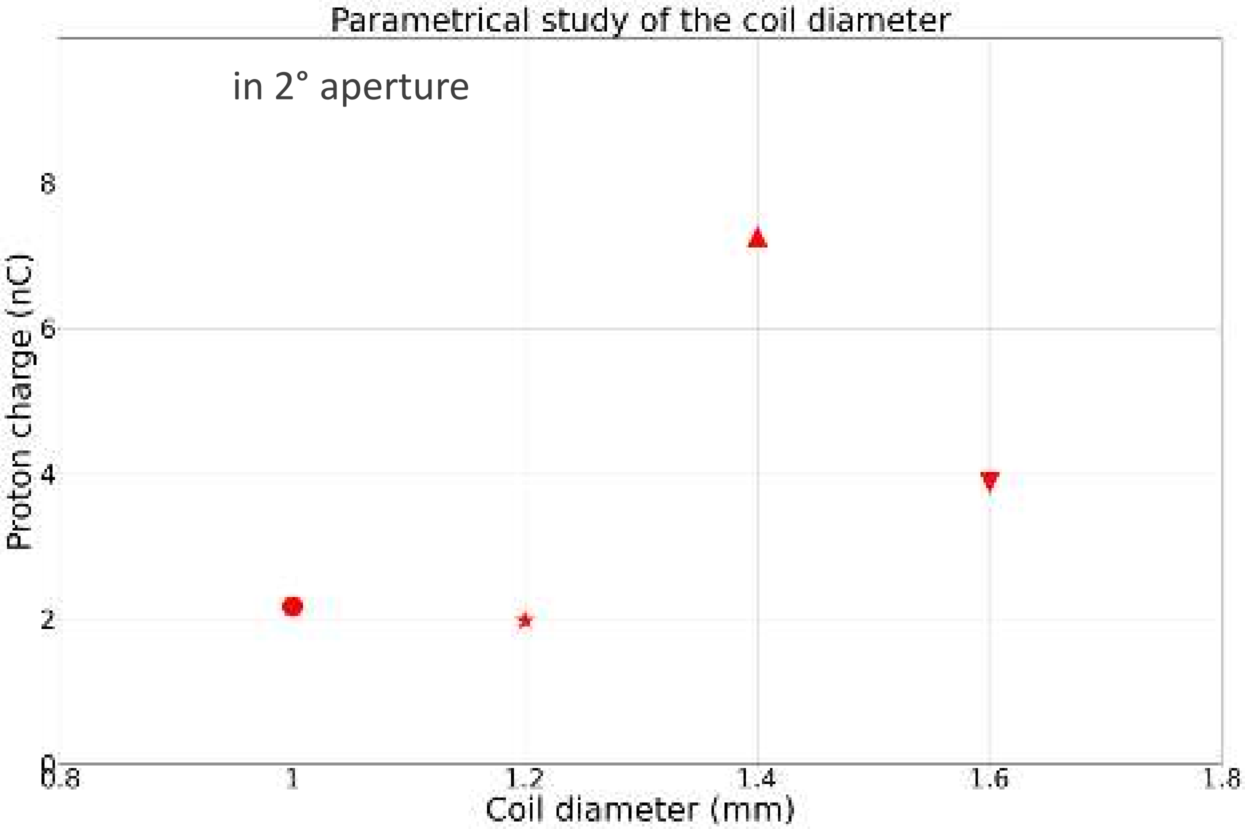

Experimental shots – p=0,4mm, L=16mm

- Spectrum of similar shape between different diameters
- Difference in the charge through the 2° cone:
  - ⇒ Maximum charge at d=1.4mm
  - ⇒ Equilibrium between proton injection and EM fields strength

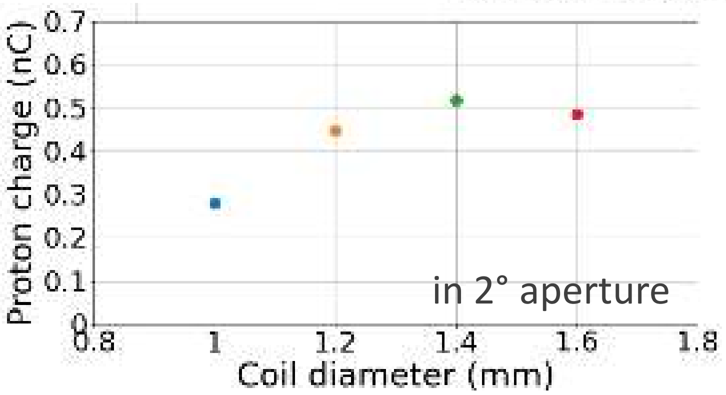

PIC simulations – p=0,4mm, L=16mm

- Qualitative agreement between experiments and simulations on the optimum diameter for proton charge
⇒ Numerical model will be used to find the optimal diameter for each coil pitch (cf poster M. Bardon)

Arthur HIRSCH – arthur.emmanuel.hirsch@protonmail.com

Outline

- Motivations and phenomenology
- Experimental set-up
- Reminder of PACMAN 1 results
- PACMAN 2 parametrical studies
- **Robustness study**
- Conclusion and perspectives for PACMAN 3 and PETAL shots

PACMAN 2: Shot-to-shot variation

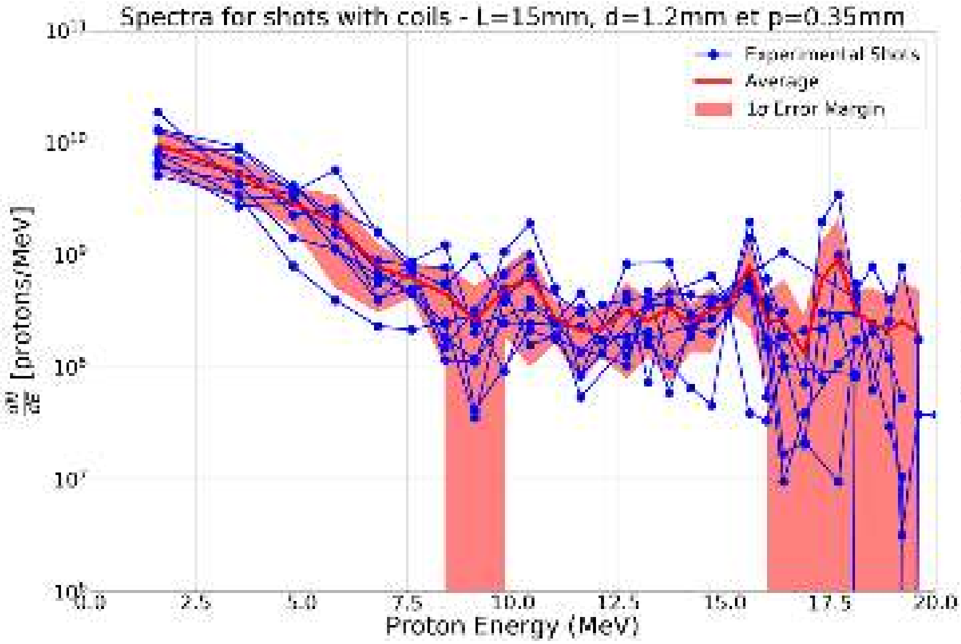

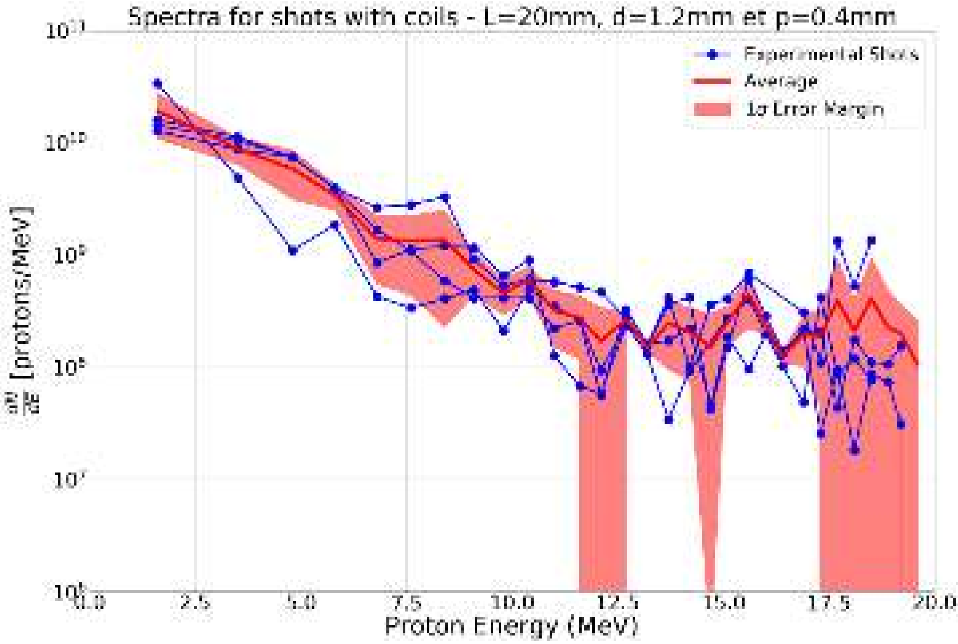

For similar targets:
- Big shot-to-shot variation
- Relatively stable under 10MeV
- Big variation over 15 MeV

Several possible sources for such variations:
- Experimental parameters (laser energy, coil-foil angle, non centered shot, etc)
  - $\Rightarrow$ Verification by PIC simulation with SOPHIE (next slides)
- Noise on the Radiochromic Films (RCF)

PACMAN 2: Robustness Study – Coil-foil distance

Coil-foil distance:
Experimentally $\Delta z = 20\text{-}100\ \mu m$

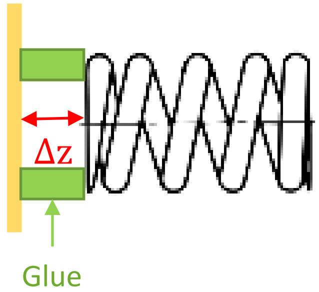

Emissive zone deviation:
Experimentally $\Delta x = 0\text{-}200\ \mu m$

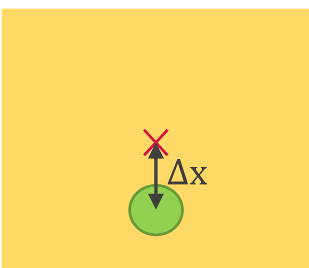

Coil-foil angle:
Experimentally $\Delta\theta = 0\text{-}5°$

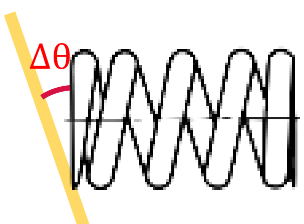

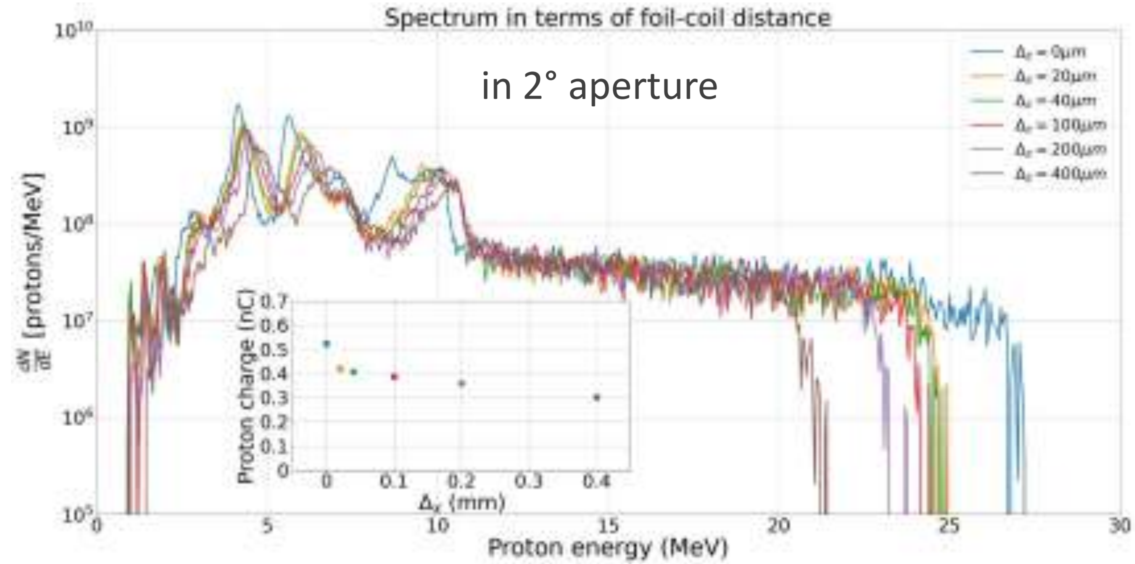

Simulation study:

⇒ No impact on the high energy plateau

⇒ Maximum energy reduced but stable

⇒ Small shift on the low energy bunches

⇒ Not coherent with the noise observed experimentally

PACMAN 2: Robustness Study – Laser energy variation

Laser energy variation:
Experimentally $\Delta E = \pm 0.3E_0$

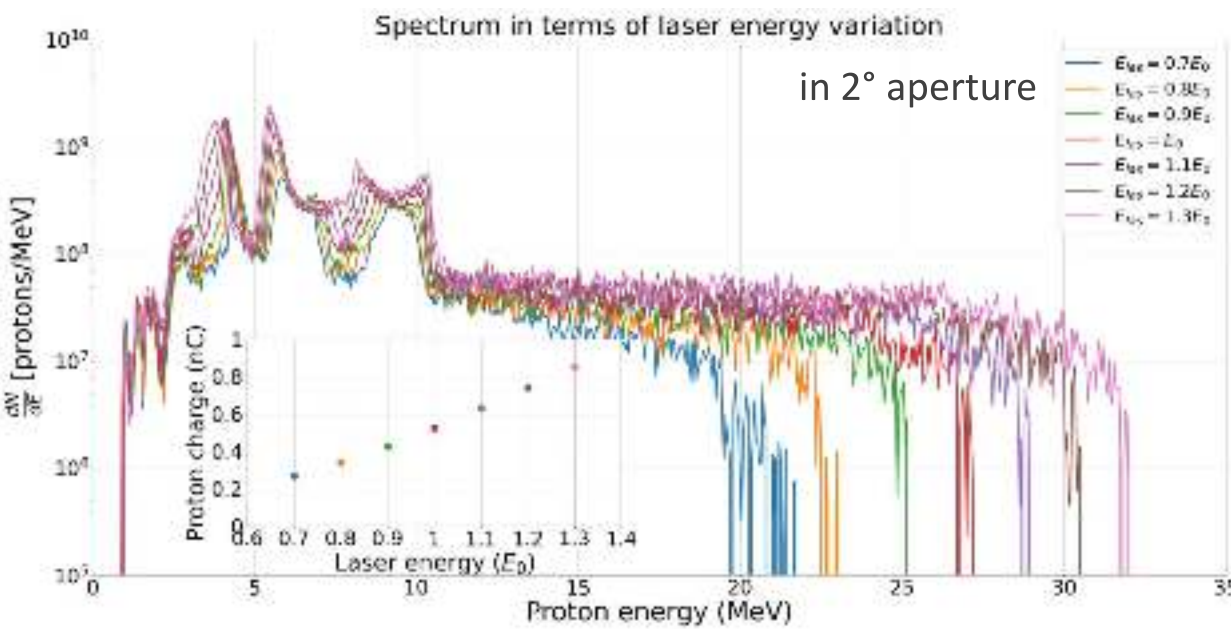

Simulation study:

⇒ Strong impact on the high energy plateau
⇒ Maximum energy strongly impacted
⇒ Small reduction of low energy bunches maximum

⇒ Potential source for the observed shot-to-shot variations

To study the impact of noise on the spectrum unfolding, we added to a GEANT4 simulated perfect RCF:

- 10-20% of each pixel value: measurement error
- Background noise measured on experimental TNSA shots

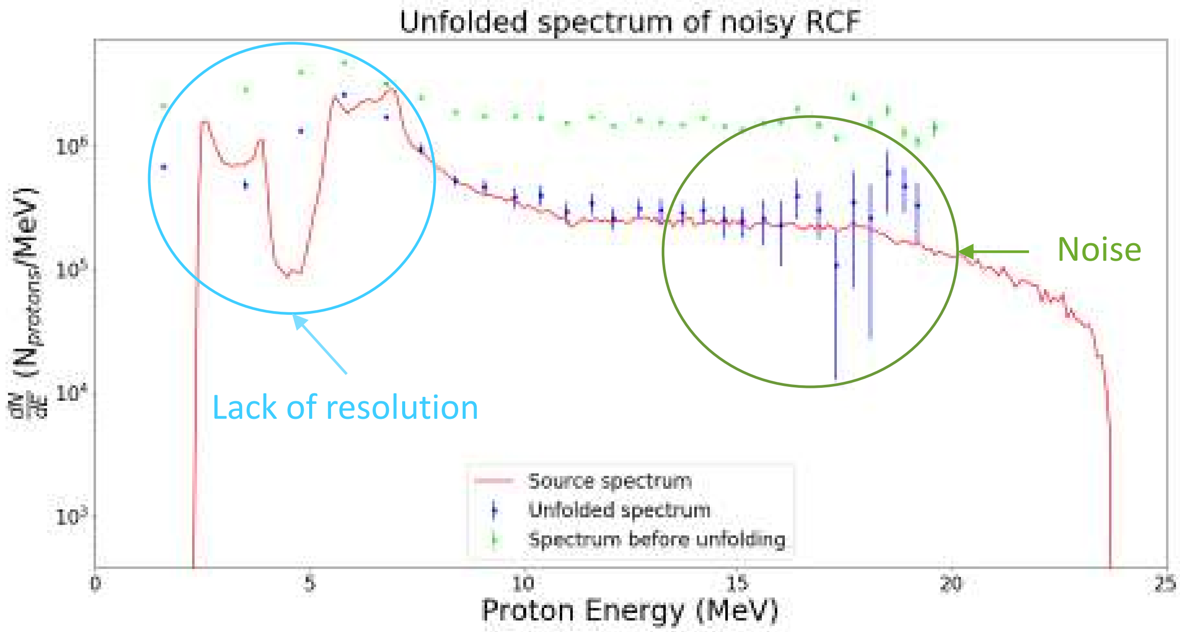

We can see that noise is strong at high energies and weak at low energies.
⇒ Potential source of our observed shot-to-shot variations

Use of Thomson parabola during next campaign
⇒ More precise and better resolution

Outline

- Motivations and phenomenology
- Experimental set-up
- Reminder of PACMAN 1 results
- PACMAN 2 parametrical studies
- Robustness study
- **Conclusion and perspectives for PACMAN 3 and PETAL shots**

Conclusion and perspectives

- PACMAN 2 campaign has confirmed PACMAN 1 results and showed several new results on the use of micro-coils to improve laser ion acceleration

- Parametrical study of PACMAN 2:

$\Rightarrow$ Presence of an optimal diameter for proton injection

$\Rightarrow$ Strong increase of the maximum proton energy from the TNSA shots for all coil lengths

- Robustness of PACMAN 2

$\Rightarrow$ 2 possible sources are identified: RCF measurements and laser energy variation

$\Rightarrow$ Thomson parabola and less laser energy variation should improve experimental results

$\Rightarrow$ Simulation results are very robust under most experimental parameters.

- Shots with variable pitch coils and variable diameter coils are still being analyzed

Conclusion and perspectives

- Paths of improvement for PACMAN 3 (2022)

⇒ Hemispherical targets for better injection

⇒ Thomson parabola for finer proton spectra

⇒ Numerical model to design optimized coils: faster than PIC simulations

- Future campaign on PETAL (2024)

⇒ Higher energy proton beams: first simulations give protons of ~100 MeV

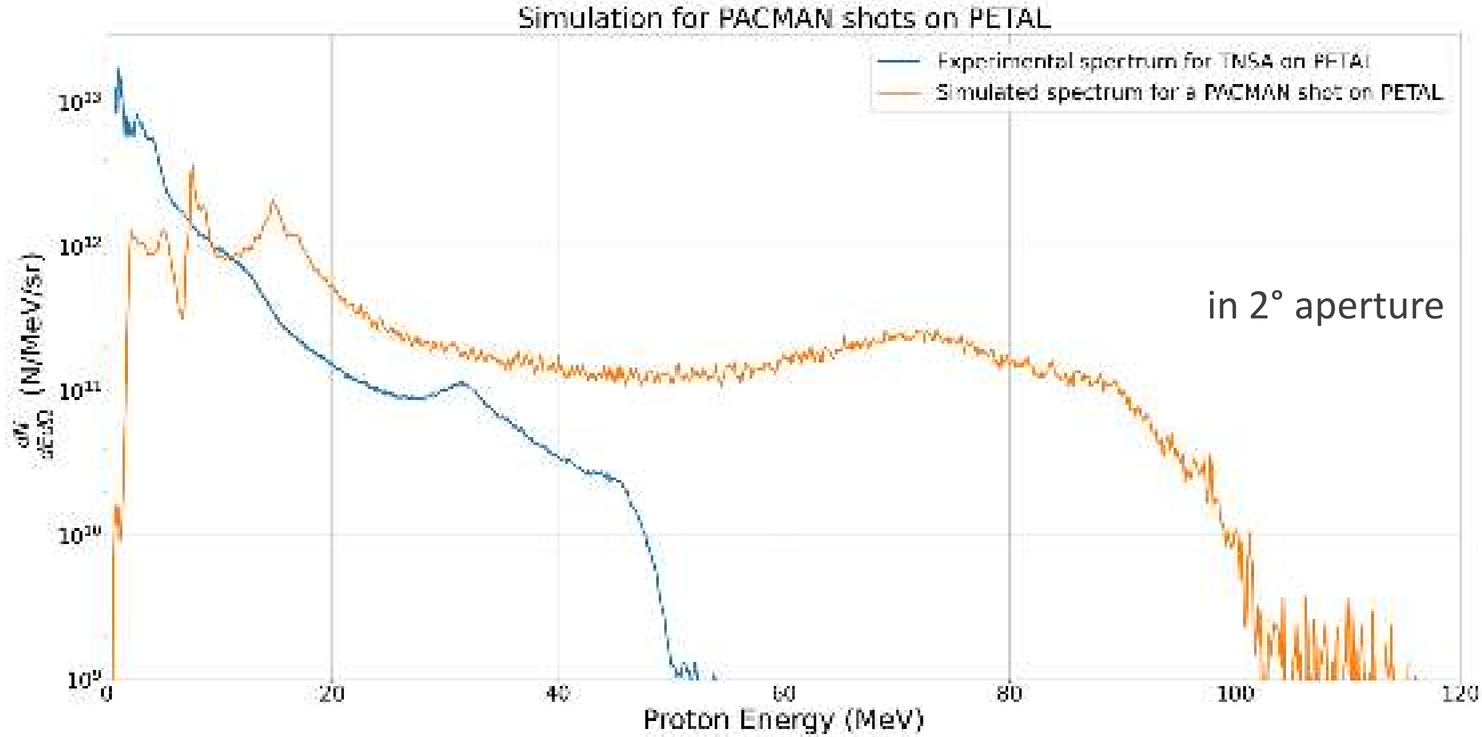

Thank you for your attention

September 30th, 2021

▶ **Arthur HIRSCH – arthur.emmanuel.hirsch@protonmail.com**

DE LA RECHERCHE À L’INDUSTRIE

Annexes

September 30th, 2021

PACMAN 2: Robustness Study – Coil-foil distance

Coil-foil distance:
Experimentally $\Delta z = 20\text{-}100\ \mu m$

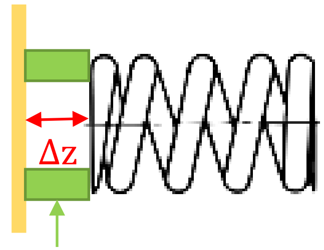

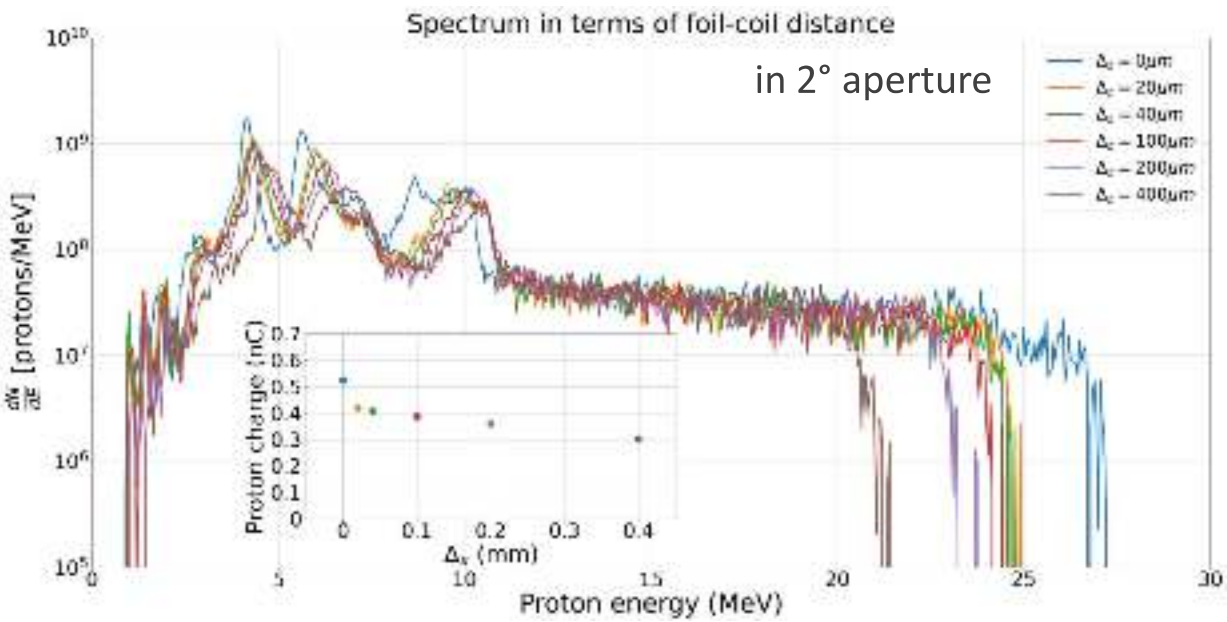

Simulation study:

⇒ No impact on the high energy plateau
⇒ Maximum energy reduced but stable from 20 to 100µm
⇒ Small shift on the low energy bunches

⇒ Not coherent with the noise observed experimentally

Emissive zone deviation:
Experimentally $\Delta x = 0\text{-}200\ \mu m$

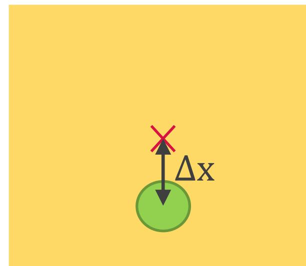

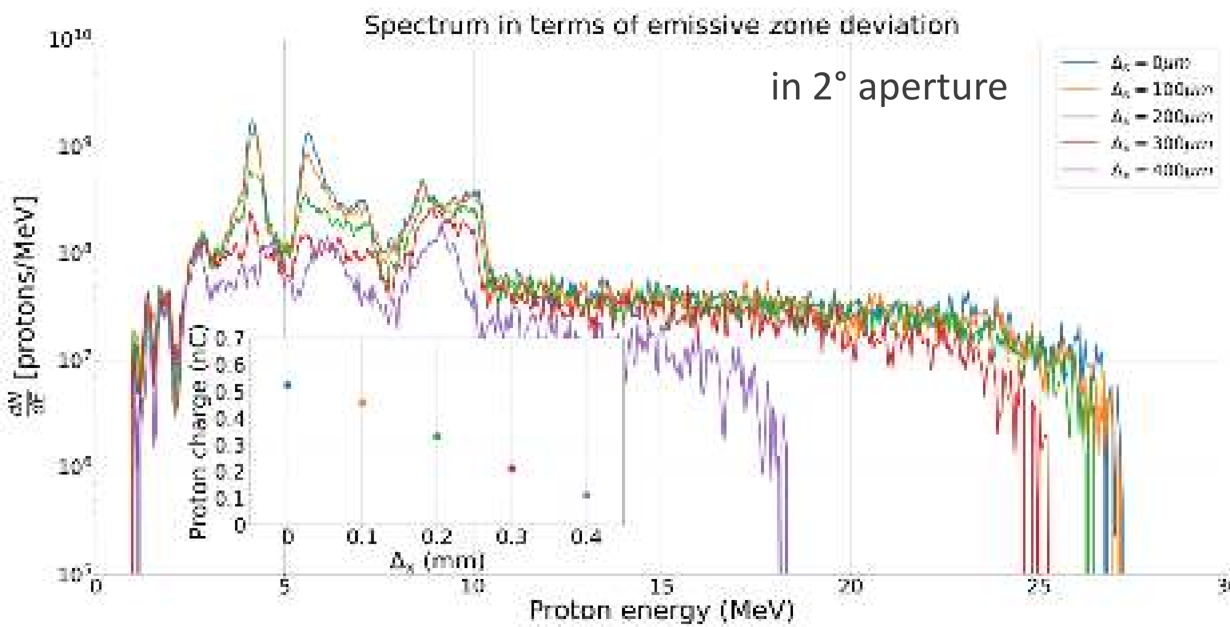

Simulation study:

⇒ No impact on the high energy plateau as long as the emission is inside the coil
⇒ Maximum energy stable
⇒ Small reduction of low energy bunches maximum

⇒ Not coherent with the noise observed experimentally

PACMAN 2: Robustness Study - Coil-foil angle

Coil-foil angle:
Experimentally $\Delta\theta = 0\text{-}5°$

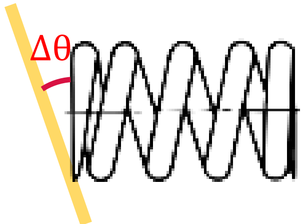

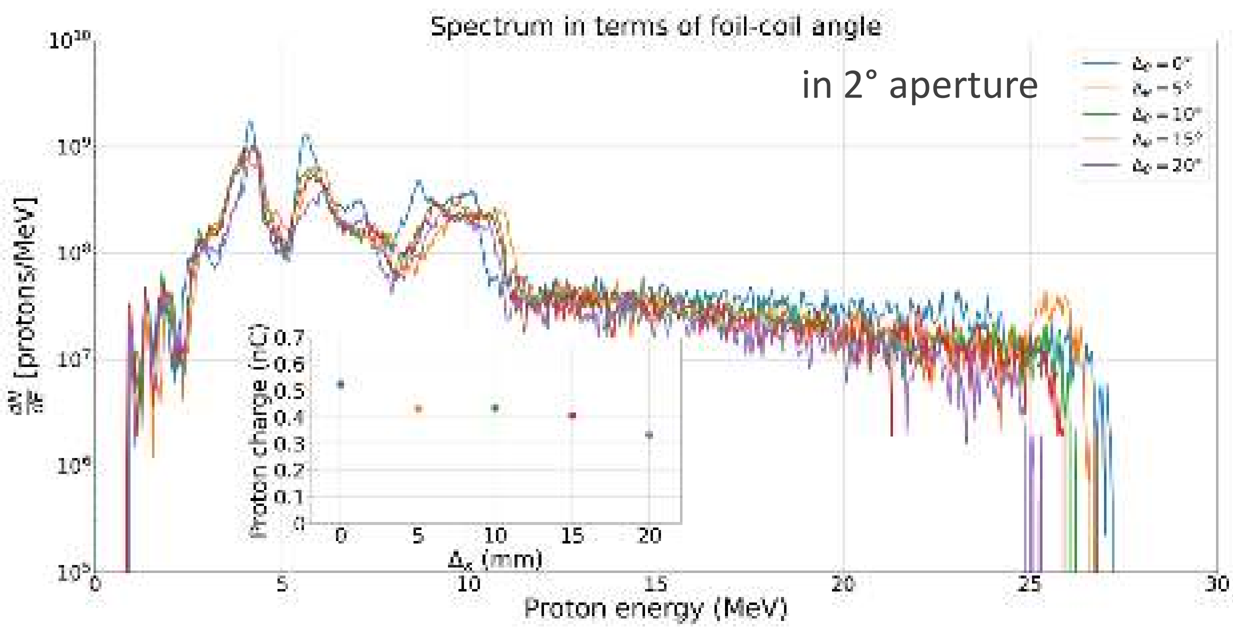

Simulation study:

⇒ Small impact on the high energy plateau
⇒ Maximum stable for a tilt under 15°
⇒ Small shifts on the low energy bunches

⇒ Not coherent with the noise observed experimentally

Numerical Parameters

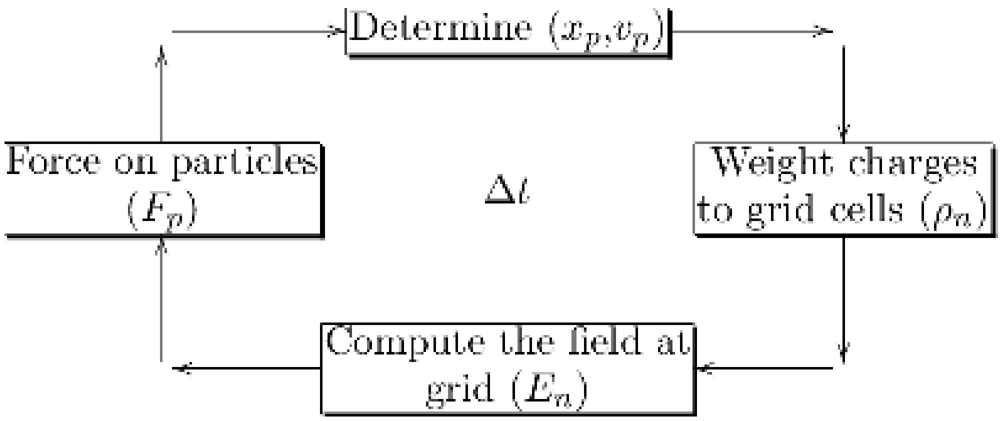

$\Delta x = 20\text{-}100\ \mu m$
$\Delta t = 3.85*10^{-14}\ s$
$= 3.85*10^{-2}\ ps$
$C*\Delta t = 11{,}5\ \mu m$

$N_p = 30*10^6$
$N_e = 60*10^6$

$N_{mailles} = 1.6*10^9$

$\tau_p = 15\ ps$
$\tau_e = 15\ ps$

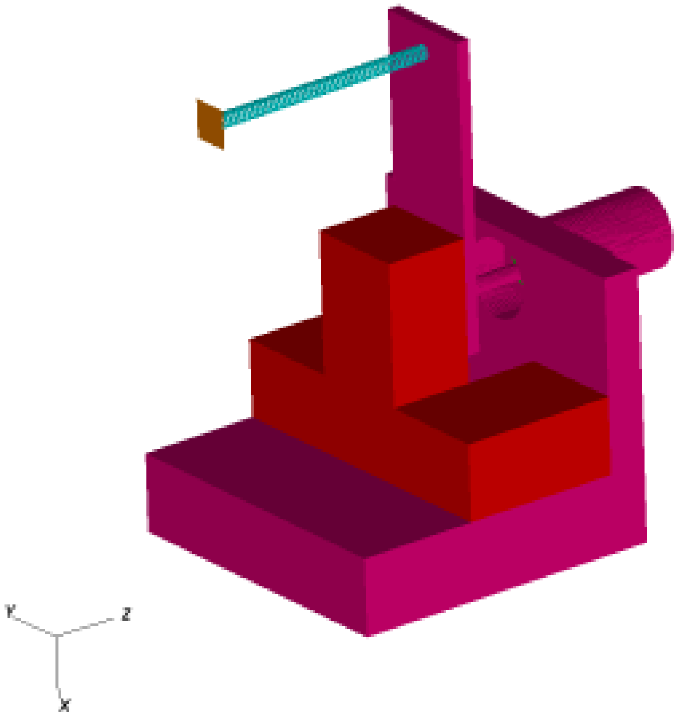

RCF unfolding

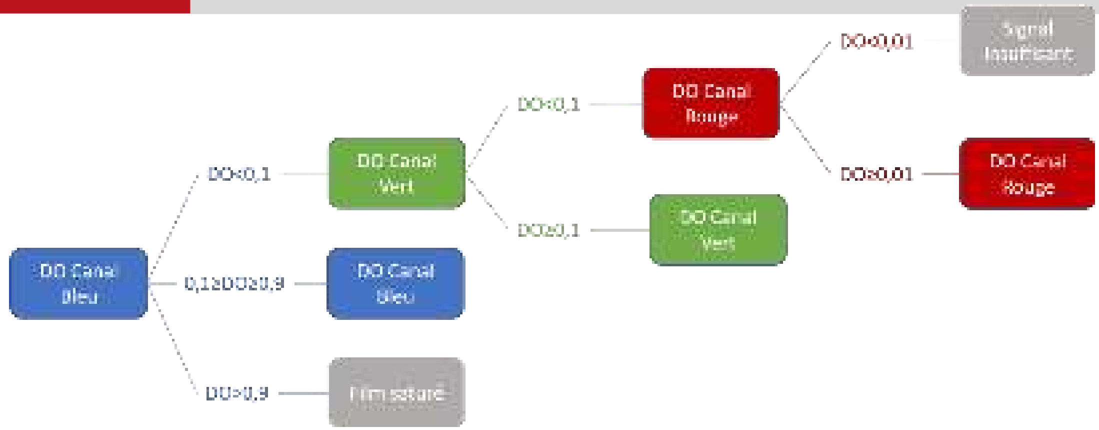

- Compute the optical density (OD) of every pixel in RGB
- Select the channel according the optical density
- Calculate the deposited energy with the following formula (A, B, C and D are calculated for each stack of RCF by the DCRE)

$$E_{dep} = exp\left(A + B \times DO^k + C \times DO + D \times DO^2\right)$$

PACMAN 2 RCF response function

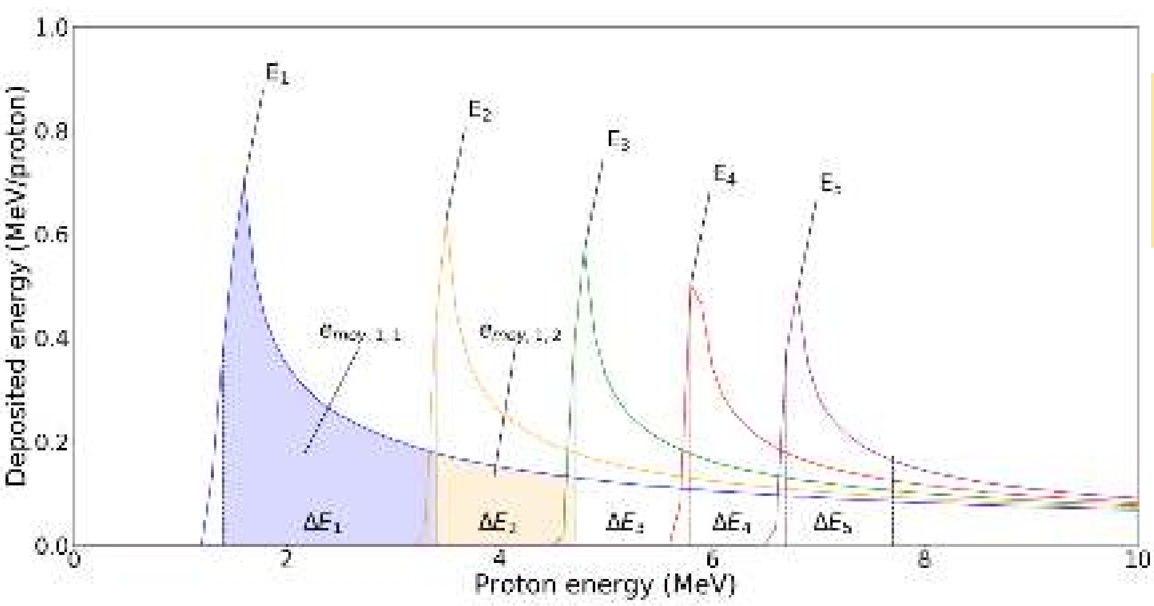

- Apply the following formula to each film starting from the last film with visible signal

$$\frac{\Delta N_i}{\Delta E_i} = \frac{\left(e_{dep,total,i} - \sum_{j=i+1}^{N} \frac{\Delta N_j}{\Delta E_j} \times e_{moy,j,i}\right)}{e_{moy,i,i}}$$

PETAL Simulations and neutron production

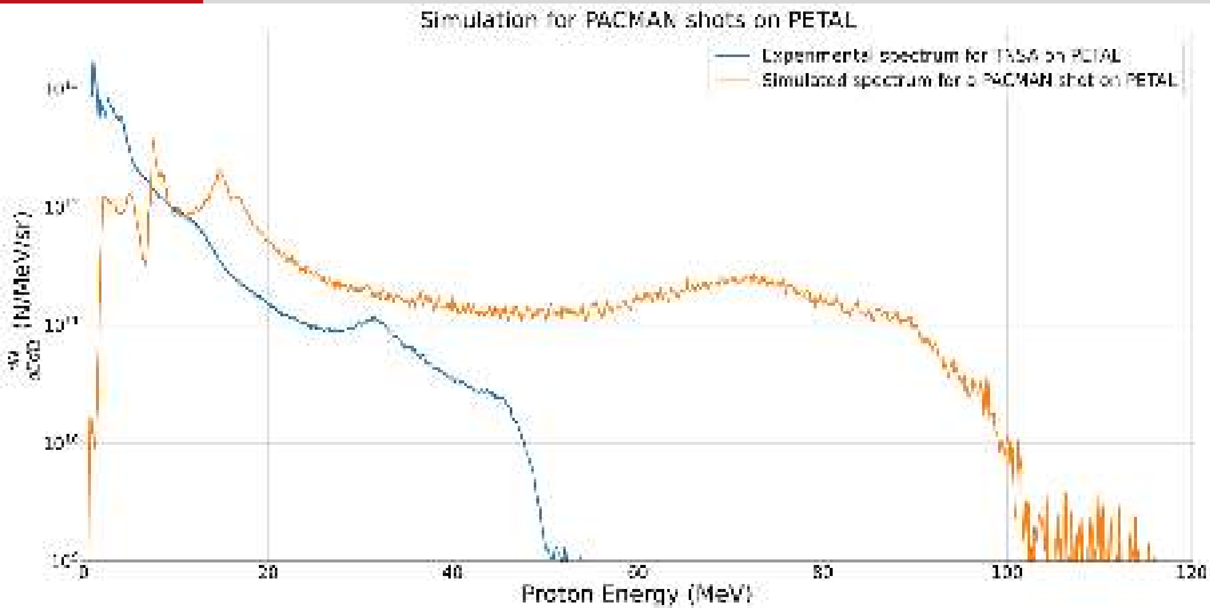

- Strong increase of the cut-off energy: from 50 to 100 MeV
- In the 2° cone, augmentation of the beam intensity

⇒ Highly energetic, highly focused proton beam

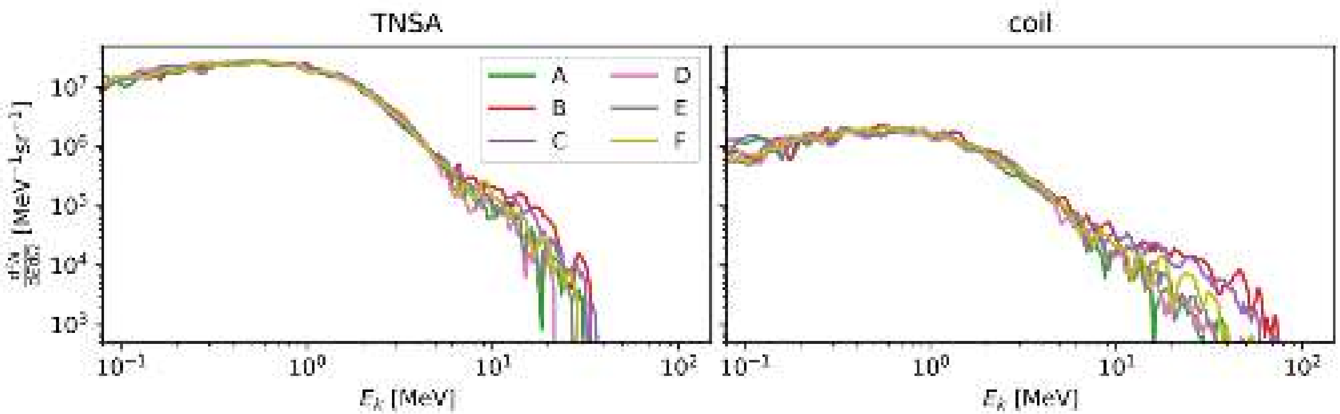

Fig: Simulated spectra of the neutrons reaching the six LMJ nTOF detectors (DP14) at their respective positions using input proton beams (left) the one produced by a simple flat target, i.e. in the TNSA regime, and (right) the one boosted by an helical coil. As a converter, 100 µm thick Pb foil has been used in both cases.